

Magnetoelectric effects in porous ferromagnetic-piezoelectric bulk composites: Experiment and theory

V. M. Petrov, G. Srinivasan, and U. Laletsin

Physics Department, Oakland University, Rochester, Michigan 48309, USA

M. I. Bichurin and D. S. Tuskov

Institute of Electronic Information Systems, Novgorod State University, B. S. Peterburgskaya Strasse 41, 173003 Veliky Novgorod, Russia

N. Paddubnaya

Institute of Technical Acoustics, National Academy of Sciences of Belarus, Ludnikov Avenue 13, 210023 Vitebsk, Belarus
(Received 16 November 2006; published 16 May 2007)

Porosity dependence of magnetoelectric (ME) parameters has been investigated in ferrite-piezoelectric bulk composites. Studies were performed on modified nickel ferrite-lead zirconate titanate. The modification involved departure from stoichiometry and the addition of cobalt oxide to the ferrite that resulted in orders of magnitude increase in the resistivity and an enhancement in the strength of ME voltage coefficient. Samples with porosity ranging from 5% to 40% were prepared. Data on low-frequency ME voltage coefficient revealed a 60%–70% decrease as the porosity p was increased from 5% to 40%. The porosity dependence was even stronger for ME coupling at electromechanical resonance: a 96% reduction in the ME voltage coefficient when p was increased from 5% to 40%. A model that considers the influence of porosity on ME interactions has been developed. The composite is assumed to consist of piezoelectric, magnetostrictive, and void (pores) subsystems. We solved combined elastostatic, electrostatic, and magnetostatic equations to obtain effective composite parameters (piezoelectric coupling, magnetostriction factors, compliances, ME coefficients). Expressions for porosity dependence of ME voltage coefficients have been obtained for low frequencies and at electromechanical resonance. The calculated ME coefficients are in very good agreement with the data.

DOI: [10.1103/PhysRevB.75.174422](https://doi.org/10.1103/PhysRevB.75.174422)

PACS number(s): 75.80.+q, 77.65.-j, 77.84.-s, 81.05.Rm

I. INTRODUCTION

In materials that are magnetoelectric, the induced polarization P is related to the magnetic field H by the expression $P = \alpha H$, where α is the second rank magnetoelectric (ME) susceptibility tensor.¹ Another parameter of importance is the ME voltage coefficient $\alpha_E = E/H$ which is related to α by the expression $\alpha = \varepsilon_o \varepsilon_r \alpha_E$, where ε_r is the relative permittivity of the material. The effect was first observed in antiferromagnetic Cr_2O_3 with a room temperature α_E of 20 mV/cm Oe.² Composites are of interest for the enhancement of ME effects.^{3,4} A composite consisting of piezomagnetic and piezoelectric phases is expected to be magnetoelectric since the ME coefficient $\alpha_E = \delta E / \delta H$ is the product of the piezomagnetic deformation $\delta z / \delta H$ and the piezoelectric field generation $\delta E / \delta z$.⁵⁻⁸

Two types of composites, bulk and layered, have been studied extensively.⁵⁻¹⁵ Bulk composites have the advantage of superior mechanical strength over layered samples. One could also easily control physical, magnetic, electrical, and ME parameters with proper choice for the two phases and their volume fractions. A key factor of importance for ME properties is the porosity in bulk composites. The strength of ME interactions depend on the mechanical connectivity between the magnetic and piezoelectric phases.⁹ The presence of pores disrupts the local connectivity and would also give rise to local demagnetization and depolarization. Porosity effects have not been considered in any detail so far. Here, we provide a systematic experimental investigation and modeling of porous bulk composites.

It is necessary to choose the appropriate bulk composite system for such a study. The ME composites of primary interest in the past were nickel or cobalt ferrite with BaTiO_3 .^{3,4} One of the necessary conditions for the existence of ME effect is the presence of electrical polarization in a sample. However, ferrites with a higher electrical conductivity than the piezoelectric phase worsen conditions for polarization and decreases the magnitude of ME effects. The primary reason for high conductivity is the possible presence of Fe^{2+} in ferrites that (i) limits the poling field leading to poor piezoelectric coupling and (ii) leakage current through the sample resulting in loss of piezoelectrically generated charges. Several studies in recent years focused on enhancing the ME effects by increasing the composite resistivity with substitutions in ferrites.^{6,7}

In this study, samples of high resistivity ferrite and piezoelectric composites have been synthesized with porosity ranging from 5% to 40%. Measurements of transverse and longitudinal ME coefficients have been carried out at 1 kHz and at electromechanical resonance (EMR). We measured a 60% reduction in the low-frequency ME voltage coefficient α_E as the porosity p is increased from 5% to 40%. The porosity dependence is much stronger for ME coupling at EMR: a 96% reduction in α_E when p is increased from 5% to 40%.

We also discuss here a model that considers the influence of porosity on ME interactions in a bulk composite. The composite is assumed to consist of piezoelectric, magnetostrictive, and void (pores) subsystems. We solved combined

elastostatic, electrostatic, and magnetostatic equations to obtain effective composite parameters (piezoelectric modules, magnetostriction factors, compliances, ME coefficients).¹⁶ Expressions for ME voltage coefficients have been obtained for low frequencies and at electromechanical resonance. The calculated ME coefficients are in very good agreement with the data.

II. COMPOSITE SYNTHESIS AND CHARACTERIZATION

Bulk composites of modified nickel ferrite, $\text{NiFe}_{1.9}\text{Co}_{0.02}\text{O}_{4-\delta}$, and lead zirconate titanate (PZT) were prepared. The Fe deficiency and the introduction of cobalt ions in the ferrite eliminate the possible formation of Fe^{2+} and increase its resistivity by orders of magnitude.^{6,7} For charge neutrality and a stable compound, one requires $\delta = 0.13$. Micron sized ferrite powder was synthesized by standard ceramic processing and mixed with commercial PZT in a ball mill. Composites with PZT concentration varying from 20 to 80 wt.% were made. The ball milled powder was mixed with a binder and green pellets were pressed using a die. The pressure applied to the sample was varied over a wide range from 700 kPa to 200 MPa to obtain samples with porosity $p=5\%–40\%$. The samples were sintered at 1200 °C for 1–2 h.

X-ray diffraction on powdered composites showed the presence of ferrite and PZT phases and indicated the absence of any impurities. Open- and closed-pore porosities for each sample were estimated from careful measurement of the density that varied from 3.4 to 5.7 g/cm³, depending on p . Measured saturation magnetization was in agreement with expected values. The samples (10 mm diameter and 1–2 mm thick) were polished and silver electrodes were deposited for electrical and ME characterization. Samples with low porosity, less than 10%, had resistivity no less than 10¹¹ Ω cm. Increasing the porosity to 40% caused a small increase of about 10%–20% in resistivity. However, the presence of Fe^{2+} leads to “electron-hopping-type” conduction and will have a much higher influence on the conductivity. The combined effect of iron deficiency and Co substitution resulted in at least 4–6 orders of magnitude increase in the composite resistivity compared to stoichiometric nickel ferrite-PZT.⁶ Samples were poled by heating to 80 °C and then an electrical field of 3–4 kV/mm was applied perpendicular to the disk plane for 30 min. As the sample was cooled to room temperature, the electrical field was slowly increased up to 5 kV/mm over a period of 1 h.

The ME voltage coefficient was measured by subjecting a poled sample to a bias field H and an ac field δH . With the sample plane assumed to be (1,2), the induced electric field δE_3 across the sample thickness was then measured for two different conditions: (i) transverse α_E or $\alpha_{E,31} = \delta E_3 | \delta H_1$ for H and δH_1 parallel to each other and the disk plane and perpendicular to δE_3 and (ii) longitudinal or $\alpha_{E,33}$ for all the three fields parallel to each other and perpendicular to the sample plane. An electromagnet was used for applying a static magnetic field. A pair of Helmholtz coils were used to generate an ac field at 1 kHz and the sample response was measured with a lock-in amplifier. Magnetoelectric coupling

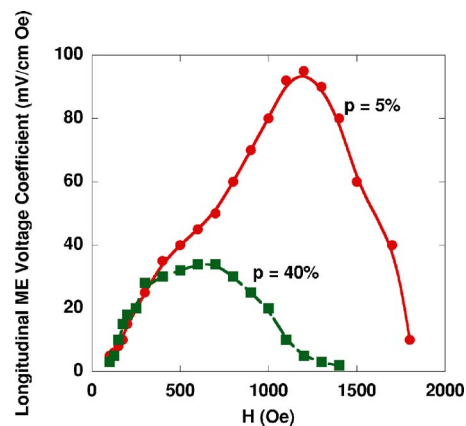


FIG. 1. (Color online) Static magnetic field H dependence of the longitudinal ME coefficient $\alpha_{E,33}$ for bulk composites of nickel ferrite and lead zirconate titanate (PZT). The data at room temperature and 1 kHz are for samples with porosity $p=5\%$ and 40% . The lines are guide for the eyes.

at EMR was measured by varying the frequency of the ac field δH over the range 100 Hz–400 kHz.

III. RESULTS

The low-frequency ME effects at 1 kHz were initially measured on composites in which the amount of PZT was increased from 20 to 80 wt %, in steps of 5%. The data revealed maximum ME effects in samples with 50 wt % ferrite and 50 wt % PZT (corresponding to approximately a 60–40 volume fraction).⁶ We then focused our attention on samples with this particular volume fraction for studies on porosity dependence of α_E . Measurements of α_E were made for longitudinal and transverse field orientations. Figure 1 shows representative data on the bias magnetic field H dependence of $\alpha_{E,33}$ for samples with $p=5\%$ and 40% . The data for longitudinal field orientations are at room temperature for $\delta H_1 = 1$ Oe at 1 kHz. One observes a general increase in $\alpha_{E,33}$ with H to a peak value, followed by a rapid drop. The voltage coefficients are directly proportional to the piezomagnetic coupling $q = d\lambda | dH$, where λ is the magnetostriction.¹⁶ The H dependence essentially follows the slope of λ vs H . When λ attains saturation, the loss of piezomagnetic coupling leads to the absence of ME effect. The peak value in $\alpha_{E,33}$ decreases from 95 mV/cm Oe for $p=5\%$ to 30 mV/cm Oe for $p=40\%$. The maximum in $\alpha_{E,33}$ occurs at a static field H_m that shows a similar variation with porosity, i.e., a decrease in H_m as p is increased.

Similar static field and porosity dependence data were obtained for the transverse ME coefficient. Figure 2 shows the porosity dependence of the maximum ME coefficients and the static field H_m at which the maxima occurs. These data are for both longitudinal and transverse field configurations. Consider the data in Fig. 2(a) for ME coefficients. For a sample with specific porosity, the longitudinal coefficient is higher than the transverse case. The coefficient $\alpha_{E,31}$ is due to in-plane magnetostrictions λ_{11} and λ_{12} , whereas $\alpha_{E,33}$ is due to $\lambda_{33} = 2\lambda_{11}$ and one ex-

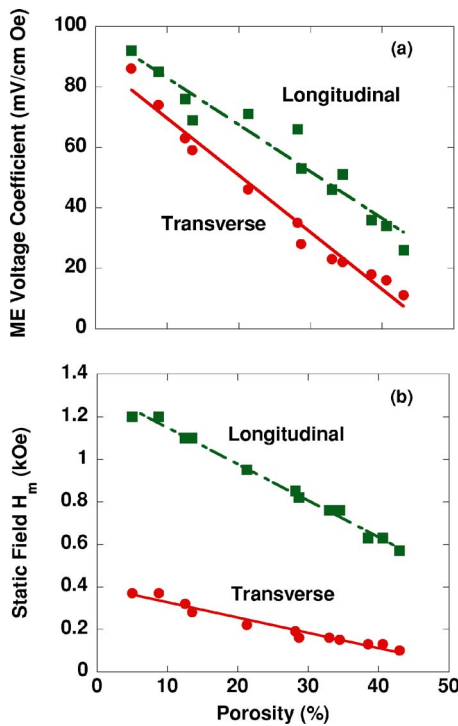


FIG. 2. (Color online) Porosity dependence of (a) maximum value of transverse and longitudinal ME coefficients and (b) the bias field H_m for maximum coupling. The data were obtained from profiles as in Fig. 1. The lines are guide for the eyes.

pects $\alpha_{E,33}=2\alpha_{E,31}$. Such an empirical relationship is confirmed in samples in the shape of cubes.⁶ The ratio of maximum longitudinal to transverse coefficient in Fig. 2(a) varies from is 1.1 for $p=5\%$ to close to 2 for $p=40\%$. Thus, a substantial deviation from the expected ratio of 2 is observed only for samples with porosities in the range 5%–20%. This can be attributed to the effect of demagnetization. At low porosity, the magnetization and the demagnetizing fields for longitudinal orientation are higher, leading to a decrease in the longitudinal ME coefficient. Consider next the p dependence of the ME coefficients in Fig. 2(a). Both coefficients show identical, linear decrease in its magnitude with increasing p . The data clearly indicate the anticipated decrease in α_E with the loss of mechanical connectivity and the consequent weakening of magnetic-mechanical-electrical interactions between the two phases with increasing p .

The variation of H_m with p in Fig. 2(b) shows features similar to p dependence of ME coefficients. It decreases by a factor of 2 for the longitudinal case when p is increased from 5% to 40%. For a specific p , the maximum in $\alpha_{E,33}$ occurs at a much higher H_m than for $\alpha_{E,31}$ and is due to the demagnetization field associated with the static field orientation for the longitudinal case. One also observes a higher slope for H_m vs p for the longitudinal case than for the transverse fields and can be attributed to the decrease in the sample magnetization and demagnetizing field with increasing p .

We also performed studies on the frequency dependence of the ME coupling. The bias field was set at H_m and the ME voltage coefficients were measured as the frequency f of the ac field δH was varied. Typical α_E vs f profiles for transverse

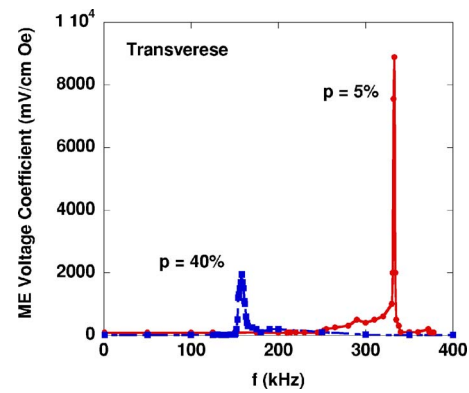


FIG. 3. (Color online) Frequency dependence of transverse ME coefficient for samples with 5% and 40% porosity. The static field was set at H_m . The lines are guide for the eyes.

fields are shown in Fig. 3. The results are for samples with $p=5\%$ and 40%. For the sample with $p=5\%$, upon increasing f , $\alpha_{E,31}$ remains small and constant for f up to 250 kHz. At higher f , one notices a rapid increase in $\alpha_{E,31}$ to a peak value of 9 V/cm Oe at 350 kHz. The peak value of $\alpha_{E,31}$ is a factor of 100 higher than the 1 kHz value and then it levels off at a much lower value. However, for $p=40\%$, the peak value is quite small and it occurs at a much lower frequency. The profile thus shows resonance with a quality factor $Q=400$ for $p=5\%$ and 100 for $p=40\%$. A similar resonance in α_E was observed for longitudinal fields. Figure 4 shows the variation in the peak ME coefficients with p . Both ME coefficients show a sharp decrease in the peak value with increasing porosity.

The profiles in Fig. 3 show the expected resonance enhancement in ME coefficients at frequencies corresponding to radial acoustic modes in the composites. Our model for the f dependence predicts giant magnetoelectric interactions at electromechanical resonance.¹⁷ We considered a sample in the form of thin disk of radius R . The ac magnetic field induces harmonic waves in the radial or thickness modes. The model considered radial modes for transverse or longitudinal fields. An averaging procedure was employed to obtain the composite parameters and the ME voltage coefficient α_E . The estimated frequency dependence of α_E showed a resonance character. The resonance frequency depends on R ,

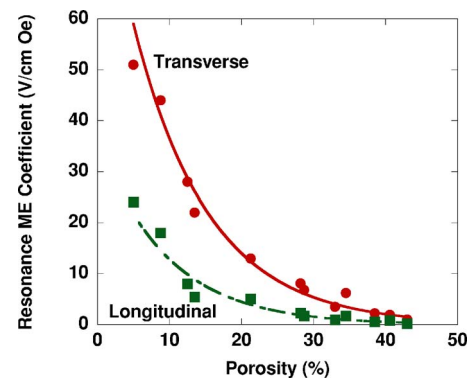


FIG. 4. (Color online) Variation of peak ME voltage coefficients with porosity. The lines are guide for the eyes.

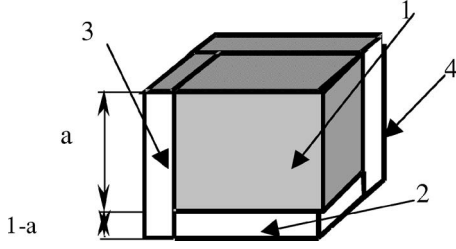


FIG. 5. Cube model of porous composite with 3-0 connectivity: 1 is a cube of air pore of side a ; 2, 3, and 4 are ferrite and piezoelectric composite units.

mechanical compliances, density, and the coefficient of electromechanical coupling. The peak value of α_E and Q are determined by the effective piezomagnetic and piezoelectric coefficients, compliances, permittivity, and loss factor.

It is clear from the data in Figs. 1–4 that the strength of ME interactions in ferrite-piezoelectric bulk composites is critically dependent on porosity. We extended our model for low-frequency and resonance ME effects to include the effect of porosity and is discussed next.^{17,18}

IV. THEORY AND COMPARISON WITH DATA

We consider a composite of ferrite and piezoelectric phases in which the pores are embedded. Dimensions of the sample are supposed to be small compared with wavelengths of ac fields involved in the measurements. The sample is assumed to have 3-0 connectivity and to consist of cubes, as in Fig. 5. One, therefore, needs to obviously analyze only one of the units to describe the whole sample. For obtaining the effective composite parameters, we use a two stage averaging procedure.² In the first stage, the composite is considered as a pore-free structure consisting of piezoelectric and magnetostrictive phases. For the polarized piezoelectric phase with the symmetry ∞m and magnetostrictive phase with the cubic symmetry, the following equations can be written for the strain, electric, and magnetic displacement:

$$\begin{aligned} {}^p S_i &= {}^p s_{ij} {}^p T_j + {}^p d_{ki} {}^p E_k, \\ {}^p D_k &= {}^p d_{ki} {}^p T_i + {}^p \varepsilon_{kn} {}^p E_n, \\ {}^m S_i &= {}^m s_{ij} {}^m T_j + {}^m q_{ki} {}^m H_k, \\ {}^m B_k &= {}^m q_{ki} {}^m T_i + {}^m \mu_{kn} {}^m H_n, \end{aligned} \quad (1)$$

where ${}^p S$, ${}^p T_j$, ${}^m S_i$, and ${}^m T_j$ are strain and stress tensor components of the piezoelectric and magnetostrictive phases, ${}^p E_k$ and ${}^p D_k$ are the vector components of electric field and electric displacement, ${}^m H_n$ and ${}^m B_k$ are the vector components of magnetic field and magnetic induction, ${}^p s_{ij}$, ${}^m s_{ij}$, ${}^p d_{ki}$, and ${}^m q_{ki}$ are compliance of the piezoelectric and magnetostrictive phases and piezoelectric and piezomagnetic coefficients, ${}^p \varepsilon_{kn}$ is the permittivity matrix, and ${}^m \mu_{kn}$ is the permeability matrix.

The pore-free bulk composite is considered as homogeneous and its behavior is described by

$${}^b S_i = {}^b s_{ij} {}^b T_j + {}^b d_{ki} {}^b E_k + {}^b q_{ki} {}^b H_k,$$

$${}^b D_k = {}^b d_{ki} {}^b T_i + {}^b \varepsilon_{kn} {}^b E_n + {}^b \alpha_{kn} {}^b H_n,$$

$${}^b B_k = {}^b q_{ki} {}^b T_i + {}^b \alpha_{kn} {}^b E_n + {}^b \mu_{kn} {}^b H_n, \quad (2)$$

where ${}^b S_i$ and ${}^b T_j$ are the average strain and stress tensor components, ${}^b E_k$, ${}^b D_k$, ${}^b H_k$, and ${}^b B_k$ are the average vector components of electric field, electric displacement, magnetic field, and magnetic induction, ${}^b s_{ij}$, ${}^b d_{ki}$, and ${}^b q_{ki}$ are effective compliance, piezoelectric, and piezomagnetic coefficients, and ${}^b \varepsilon_{kn}$, ${}^b \mu_{kn}$ and ${}^b \alpha_{kn}$ are effective permittivity, permeability, and ME coefficient. Effective parameters of the pore-free composite are obtained for the cube model, taking into account the following boundary conditions:

$${}^1 S_1 = {}^2 S_1, \quad {}^1 S_2 = {}^2 S_2, \quad {}^2 S_1 = {}^3 S_1, \quad {}^3 S_3 = {}^4 S_3,$$

$$a {}^1 S_3 + (1-a) {}^2 S_3 - {}^3 S_3 = 0, \quad a {}^2 S_2 + (1-a) {}^3 S_2 - {}^4 S_2 = 0,$$

$${}^1 A_1 {}^1 T_1 + {}^2 A_1 {}^2 T_1 + {}^3 A_1 {}^3 T_1 = 0, \quad {}^4 T_1 = 0,$$

$${}^3 A_2 {}^3 T_2 + {}^4 A_2 {}^1 T_2 = 0, \quad {}^1 A_2 {}^1 T_2 + {}^2 A_2 {}^2 T_2 = {}^3 A_2 {}^3 T_2,$$

$${}^1 T_3 - {}^2 T_3 = 0,$$

$${}^2 A_3 {}^2 T_3 + {}^3 A_3 {}^3 T_3 + {}^4 A_3 {}^4 T_3 = 0,$$

$$a {}^1 E_3 + (1-a) {}^2 E_3 - {}^3 E_3 = 0, \quad {}^3 E_3 - {}^4 E_3 = 0,$$

$${}^1 D_3 - {}^2 D_3 = 0, \quad {}^2 A_3 {}^2 D_3 + {}^3 A_3 {}^3 D_3 + {}^4 A_3 {}^4 D_3 = D_3,$$

$$a {}^1 H_3 + (1-a) {}^2 H_3 - {}^3 H_3 = 0, \quad {}^3 H_3 - {}^4 H_3 = 0,$$

$${}^1 B_3 - {}^2 B_3 = 0, \quad {}^2 A_3 {}^2 B_3 + {}^3 A_3 {}^3 B_3 + {}^4 A_3 {}^4 B_3 = B_3, \quad (3)$$

where ${}^i S_j$, ${}^i T_j$, ${}^i E_j$, ${}^i D_j$, ${}^i H_j$, and ${}^i B_j$ denote strain, stress, electric field, and displacement, magnetic field, and induction components, respectively, and ${}^i A_j$ is cross-section area of the i th unit perpendicular to direction j . For finding the effective parameters for pore-free composite, we solve Eqs. (4) for strains, stresses, and electric and magnetic fields taking into account Eqs. (1). Substituting the obtained solutions into Eqs. (2) gives the required parameters. Analytical expressions for effective composite parameters are too tedious and the equations were solved numerically. Following Ref. 18, we used for NFO-PZT bulk composite the 3-0 model that is more appropriate as compared with the 0-3 model. Clamping caused by neighboring units was taken into account using the expression ${}^b S_i = -{}^b s_{ii} {}^b T_i$.

In the second stage of the averaging procedure, the porous composite is considered as a structure consisting of ferrite-piezoelectric composite (units 2–4 in Fig. 5) and air pores (unit 1). For an air pore, the strains ${}^a S_i$ and electric ${}^a D_k$ and magnetic ${}^a B_k$ inductions are related to stress components ${}^a T_j$ and magnetic ${}^a H_n$ and electric ${}^a E_n$ fields as follows:

$$\begin{aligned}
 {}^a S_i &= {}^a s_{ij} {}^a T_j, \\
 {}^a D_k &= {}^a \varepsilon_{kn} {}^a E_n, \\
 {}^a B_k &= {}^a \mu_{kn} {}^a H_n,
 \end{aligned} \quad (4)$$

where ${}^a s_{ij}$ is compliance, ${}^a \varepsilon_{kn}$ is the permittivity matrix, and ${}^a \mu_{kn}$ is the permeability matrix. Here, compliance of unit 1 (Fig. 5) is assumed to be considerably greater compared to units 2–4.

In case of longitudinal ME effect, the composite is poled with an electric field E along direction 3. The bias field H and the ac field δH are along the same direction and the resulting induced electric field δE is estimated across the sample thickness. The boundary conditions for this case are similar to Eqs. (3). Effective parameters of the porous composite are obtained by solving Eqs. (2)–(4) and the open circuit condition: ($D_3=0$). Here, D_3 is the average electric displacement in the porous composite. Then, we find an expression for $\alpha_{E,L} = \alpha_{E,33} = \delta E_3 / \delta H_3$.

For theoretical estimates of the low-frequency ME coefficients the following parameters were assumed: for PZT,

$${}^p s_{11} = 15.3 \times 10^{-12} \text{ m}^2/\text{N}, \quad {}^p s_{12} = -5 \times 10^{-12} \text{ m}^2/\text{N},$$

$${}^p s_{13} = -7.22 \times 10^{-12} \text{ m}^2/\text{N},$$

$${}^p s_{33} = 17.3 \times 10^{-12} \text{ m}^2/\text{N}, \quad {}^p d_{31} = -175 \times 10^{-12} \text{ m/V},$$

$${}^p d_{33} = 400 \times 10^{-12} \text{ m/V}, \quad {}^p \varepsilon_{33}/\varepsilon_0 = 1750.$$

and for ferrite:

$${}^m s_{11} = 6.5 \times 10^{-12} \text{ m}^2/\text{N}, \quad {}^m s_{12} = -2.4 \times 10^{-12} \text{ m}^2/\text{N},$$

$${}^m q_{31} = 125 \times 10^{-12} \text{ m/A},$$

$${}^m q_{33} = -680 \times 10^{-12} \text{ m/A}, \quad {}^m \mu_{33}/\mu_0 = 3, \quad {}^m \varepsilon_{33}/\varepsilon_0 = 10.$$

Calculated dependence of low-frequency ME voltage coefficients on porosity is shown in Fig. 6 for nickel ferrite-PZT bulk composite. The estimates are for a 60–40 ferrite-PZT volume fraction and for longitudinal fields. Measured values of $\alpha_{E,33}$ (Fig. 2) are shown for comparison. The theory predicts a decrease in $\alpha_{E,33}$ with increasing porosity. Although the theory is for a specific connectivity of 3–0, it is quite remarkable that there is excellent agreement with the data.

Next, we consider the ME interactions at EMR. Porosity is expected to influence the ME coupling through two mechanisms. First, the growth of pores causes a decrease in the effective piezoelectric and piezomagnetic coefficients. The ME voltage coefficient for radial mode is determined by the effective piezoelectric and piezomagnetic coefficients of the composite and may be described by¹⁷

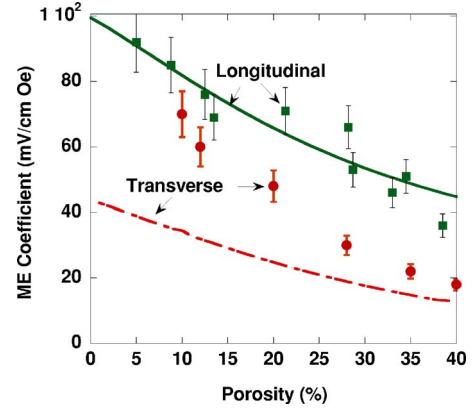


FIG. 6. (Color online) Estimated porosity dependence of ME voltage coefficient for 60% nickel ferrite-40% PZT bulk composite. The squares (circles) are data for longitudinal (transverse) ME coefficient from Fig. 2. The lines are theoretical values.

$$\alpha_{E,T} = \frac{1}{\Delta_a} \left\{ \frac{d_{31}(q_{11} + q_{12})}{\varepsilon_{33}s_{11}(1-\nu)} \left[1 - \frac{(1+\nu)J_1(\kappa)}{\Delta_r} \right] - \frac{m_{31}}{\varepsilon_{33}} \right\}, \quad (5)$$

where $\Delta_r = \kappa J_0(\kappa) - (1-\nu)J_1(\kappa)$, $\Delta_a = 1 - K_p^2 + K_p^2(1+\nu)J_1(\kappa)/\Delta_r$, $K_p^2 = 2d_{31}^2/[\varepsilon_{33}s_{11}(1-\nu)]$, $J_0(\kappa)$ and $J_1(\kappa)$ are Bessel functions of the first kind, $\kappa = kR$, $k = \sqrt{\rho s_{11}(1-\nu^2)\omega}$, q_{ij} and d_{ij} are piezomagnetic and piezoelectric coefficients, ε_{ij} is permittivity matrix, m_{33} is the ME susceptibility, $\nu = -s_{12}/s_{11}$ is the Poisson's ratio, ρ is the density, and ω is the angular frequency.

The second mechanism of importance is that the pores make damp the elastic vibrations and increase the loss of energy and broaden the resonance line, leading to further decreasing the ME coefficient. This decrease is taken in to account in Δ_a through the loss factor $\Gamma = 1/Q$, where Q is the measured quality factor of EMR. The frequency dependence shows very significant enhancement in ME coupling at electromechanical resonance for radial modes in the porous composite. Estimated dependence of ME voltage coefficients at EMR on pore volume fraction is shown in Fig. 7 and is

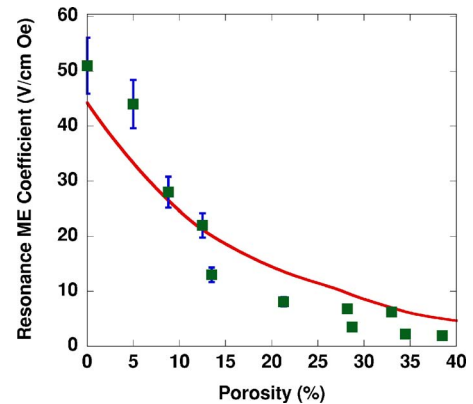


FIG. 7. (Color online) Porosity dependence of transverse ME voltage coefficient at EMR for the bulk composite. The squares are data points.

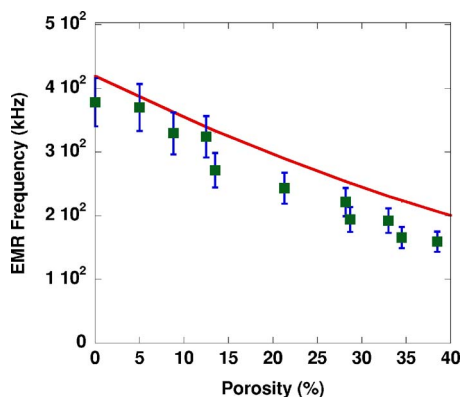


FIG. 8. (Color online) Porosity dependence of EMR frequency for the bulk composite. The circles are data points.

compared with data. There is very good agreement between theory and data.

Finally, we consider the variation with porosity of the EMR frequency for radial mode that can be found by setting $\Delta_\omega=0$ [Eq. (5)]. One anticipates a decrease in EMR frequency with increasing porosity due to changes in the effective compliance s_{11} and density ρ . The effective compliance s_{11} is determined from Eqs. (2)–(4) and ρ is the measured density. Figure 8 shows the estimated variation in the EMR frequency along with the data. It is clear that agreement between theory and data is quite good.

V. CONCLUSION

The influence of porosity on magnetoelectric interactions has been investigated in bulk composites consisting of modified nickel ferrite and PZT. The modification of ferrite included Co substitution and Fe deficiency that resulted in high resistivity for the ferrite and an enhancement in ME voltage. Composites with 60 vol. % ferrite and 40 vol. % PZT were made with porosity varying from 5% to 40%. Measurements of low-frequency ME coefficients indicated a linear decrease its magnitude with increasing p . A similar but a much sharper decrease in the ME voltage with p was measured at electromechanical resonance due to radial acoustic modes. A theoretical model has been proposed for a porous composite. Estimates of porosity dependence of ME voltage coefficients at 1 kHz and at EMR and frequency of radial modes are in very good agreement with the data.

The results presented here are of practical importance for achieving bulk composite with desired ME parameters.

ACKNOWLEDGMENTS

The work at Oakland University was supported by NSF grants (DMR-0606153, NIRT-0609377, and ECCS-0621907). The work at Novgorod State University was supported by the Russian Foundation for Basic Research (Projects No. 06-08-00896-a, No. 06-02-08071-ofi, and No. 05-02-39002-GFEN-a).

¹L. D. Landau and E. M. Lifshitz, *Electrodynamics of Continuous Media* (Pergamon, Oxford, 1960), p. 119 (translation of Russian edition, 1958).

²D. N. Astrov, *Sov. Phys. JETP* **13**, 729 (1961).

³J. Van den Boomgaard, D. R. Terrell, and R. A. J. Born, *J. Mater. Sci.* **9**, 1705 (1974).

⁴J. Van den Boomgaard, A. M. J. G. van Run, and J. Van Suchtelen, *Ferroelectrics* **14**, 727 (1976).

⁵J. Ryu, A. V. Carazo, K. Uchino, and H. Kim, *J. Electroceram.* **7**, 17 (2001).

⁶V. M. Laletin and G. Srinivasan, *Ferroelectrics* **280**, 177 (2002).

⁷C. P. DeVreugd, C. S. Flattery, and G. Srinivasan, *Appl. Phys. Lett.* **85**, 2550 (2004).

⁸Ce-Wen Nan and D. R. Clarke, *J. Am. Ceram. Soc.* **80**, 1333 (1997).

⁹G. Harshe, J. P. Dougherty, and R. E. Newnham, *Int. J. Appl. Electromagn. Mater.* **4**, 161 (1993).

¹⁰G. Harshe, J. P. Dougherty, and R. E. Newnham, *Int. J. Appl. Electromagn. Mater.* **4**, 145 (1993); M. Avellaneda and G. Harshe, *J. Intell. Mater. Syst. Struct.* **5**, 501 (1994).

¹¹G. Srinivasan, E. T. Rasmussen, J. Gallegos, R. Srinivasan, Yu. I. Bokhan, and V. M. Laletin, *Phys. Rev. B* **64**, 214408 (2001).

¹²K. Mori and M. Wuttig, *Appl. Phys. Lett.* **81**, 100 (2002).

¹³S. Dong, J. F. Li, and D. Viehland, *Philos. Mag. Lett.* **83**, 769 (2003).

¹⁴S. Dong, J. Zhai, F. Bai, J. F. Li, and D. Viehland, *Appl. Phys. Lett.* **87**, 062502 (2005).

¹⁵N. Cai, C. W. Nan, J. Zhai, and Y. Lin, *Appl. Phys. Lett.* **84**, 3516 (2004).

¹⁶M. I. Bichurin, V. M. Petrov, Yu. V. Kiliba, and G. Srinivasan, *Phys. Rev. B* **66**, 134404 (2002).

¹⁷M. I. Bichurin, D. A. Filippov, V. M. Petrov, V. M. Laletsin, N. Paddubnaya, and G. Srinivasan, *Phys. Rev. B* **68**, 132408 (2003).

¹⁸V. M. Petrov, M. I. Bichurin, V. M. Laletin, N. Paddubnaya, and G. Srinivasan, *Magnetoelectric Interaction Phenomena in Crystals*, NATO Science Series II, Vol. 164, edited by M. Fiebig, V. V. Eremanko, and I. E. Chupis (Kluwer Academic, London, 2004), pp. 65–70.